University of Bath

Alternative formats

If you require this document in an alternative format, please contact:
openaccess@bath.ac.uk

1 **The effect of particle size of inhaled tobramycin dry powder on the eradication of**

2 *Pseudomonas aeruginosa* **biofilms**

3

4 Reham Aljalamdeh, Robert Price, Matthew D. Jones, and Albert Bolhuis*

5

6 Department of Pharmacy and Pharmacology, University of Bath, Bath BA2 7AY, United

7 Kingdom

8

9 *Corresponding author: email: a.bolhuis@bath.ac.uk, phone +44 (0)1225 383813

Abstract

Pseudomonas aeruginosa is the predominant opportunistic bacterium that causes chronic respiratory infections in cystic fibrosis (CF) patients. This bacterium can form biofilms, which are structured communities of cells encased within a self-produced matrix. Such biofilms have a high level of resistance to multiple classes of antibiotics. A widely used treatment of *P. aeruginosa* lung infections in CF patients is tobramycin dry powder inhalation. The behaviour of particles in the lung has been well studied, and dry powder inhalers are optimised for optimal dispersion of the drug into different zones of the lung. However, one question that has not been addressed is whether the size of an antibiotic particle influences the antibiofilm activity against *P. aeruginosa*. We investigated this by fractionating tobramycin particles using a Next Generation Impactor (NGI). The fractions obtained were then tested in an *in vitro* model on *P. aeruginosa* biofilms. The results indicate that the antibiofilm activity of tobramycin dry powder inhaler can indeed be influenced by the particle size. Against *P. aeruginosa* biofilms of two clinical isolates, smaller tobramycin particles (aerodynamic diameter <2.82 μm) showed better efficacy by approximately 20% as compared to larger tobramycin particles (aerodynamic diameter <11.7 μm) However, this effect was only observed when biofilms were treated for 3 hours, whereas there was no difference after treatment for 24 hours. This suggests that in our model the rate of dissolution of larger particles limits the effectiveness of tobramycin over a 3-hour time period, which is relevant as this is equivalent to the time in which most tobramycin is cleared from the lung.

1. Introduction

In patients with cystic fibrosis (CF), the opportunistic pathogen *Pseudomonas aeruginosa* is a major cause of lung infections leading to increased morbidity and mortality rates among these patients. This is attributed partially to the ability of this bacterium to form biofilms (Ciofu et al., 2015; Muheim et al., 2017; Nikaido and Pagès, 2012). These biofilms are highly organized communities of cells that are attached to each other and/or to surfaces, and embedded within a self-synthesized extracellular polymeric substance (EPS) matrix, mainly containing extracellular DNA, polysaccharides, and/or proteins (Furiga et al., 2015). Biofilms are characterized by a high tolerance to both immune defensive mechanisms and to most of the available antibiotic therapies. For instance, it is assumed that cells inside biofilms are 10-1000 times less susceptible to anti-microbial therapies as compared to planktonic free-floating cells (Marshall et al., 2016; Patton et al., 2010; She et al., 2018).

P. aeruginosa biofilms in CF lungs settle and localise in a thick mucus layer in the trachea-bronchial region of the respiratory airways (Geller et al., 2011). Such a location makes the treatment of these infections using the systemic delivery of antibiotic agents challenging, as high doses are required to reach the lung tissue which can lead to adverse reactions. Therefore, the pulmonary delivery of antibiotics is an attractive approach for the treatment of lung CF infections (Geller et al., 2011; Worlitzsch et al., 2002). Inhaled antibacterial drugs that are used in the treatment of *P. aeruginosa* CF lung infections are in two forms, being either nebulized solutions or dry powder formulations (Ambrus et al., 2018). The currently approved inhaled dry powder antibiotics are colistin and tobramycin. For instance, TOBI Podhaler® is an approved dry powder inhalation formulation of tobramycin (McKeage, 2013; Akkerman-Nijland et al, 2020), which most CF patients prefer when comparing to nebulised tobramycin, leading to, for instance, better adherence (Harrison et al., 2014). Tobramycin powder from a capsule is aerosolized using the Podhaler device by the energy of the patient's own inspiration

58 (Konstan et al., 2011), resulting in the particles in the powder being separated from each other

59 and carried in the airstream to the lungs where they deposited.

60 Following inhalation, these particles distribute and deposit into different compartments of the

61 lung. Briefly, the lung can be divided into two regions, the conducting and the respiratory

62 zones. The conducting zone includes trachea, bronchi, bronchioles, and terminal bronchioles,

63 whereas the respiratory zone comprises of the respiratory bronchioles, alveolar ducts and

64 alveolar sacs (Hoiby, 2011). Deposition of dry powder particles in these zones depends on

65 several variables such as patient-associated factors, the inhaler device and inhaled powder

66 formulation properties (Tiddens et al., 2014) such as particle shape, density and size.

67 Drug particle size is one of the important properties that can influence both the deposition and

68 fate of particles in the respiratory airways. Normally, inhaled drug particles are polydisperse

69 in nature with a large particle size range (Deng et al., 2018). Particles with an aerodynamic

70 diameter (d_{ae}) larger than 10 µm are mostly deposited in the oropharyngeal region and do not

71 reach the lungs, and those that are between 3-10 µm are mostly deposited in the trachea-

72 bronchial region. Furthermore, particles at a range of 1-3 µm target the alveolar zone of the

73 lungs (Geller et al., 2011; Nafee et al., 2014; Verbanck et al., 2006), but those that even smaller

74 (<1 µm) are exhaled due to low inertial and gravitational forces which are insufficient to

75 deposit them (Nafee et al., 2014). Once deposited, the particles must dissolve and the rate of

76 this depends on the size of these particles, which in turn can influence drug efficacy (Nafee et

77 al., 2014).

78 Currently, studies that evaluate the *in vitro* activity of tobramycin rely on testing its efficacy

79 against *P. aeruginosa* biofilms in an aqueous solution. However, there are no biofilm models

80 to test dry powder formulations, and it is thus unclear what the effect of, for instance, particle

81 size is on antibiofilm activity, highlighting the need for a model that can address such issues.

82 To achieve this, we used a Next Generation Impactor (NGI), which is an instrument used to

4

83 measure *in vitro* behaviour of inhalable dry powder products (Rowland et al., 2018). The NGI

84 sequentially separates drug aerosols into various size categories from larger to smaller particles

85 on the basis of the particles' aerodynamic diameter (Guo et al., 2008; Roberts and Mitchell,

86 2013; Wang et al., 2017). The cut-off aerodynamic diameters of these particles were previously

87 determined at flow rates of 30 and 60 L/min (Marple et al., 2003). Using the NGI and a recently

88 developed aerosol dose collection apparatus, we fractionated tobramycin particles into

89 different sizes and tested these on a *P. aeruginosa* biofilm models to (a), test the feasibility of

90 analysing dry powders on biofilms and (b), to further understand the role of particle size on

91 antibiotic efficacy, which could be very valuable for improving the pharmacological activity

92 of inhaled antibiotics.

2. Materials and Methods

2.1 Chemicals

All chemicals and culture media were purchased from Sigma-Aldrich (Gillingham, UK) or Fisher Scientific (Loughborough, UK), unless stated otherwise. The TOBI Podhaler® and 28 mg tobramycin inhalation powder (TIP) capsules were purchased from Novartis Pharmaceuticals (Camberley, UK). Tobramycin that was used to determine the minimal inhibitory concentration (section 2.3) and a calibration curve (section 2.8) was purchased from Fisher Scientific (97% purity).

2.2 Bacterial strains and growth media

The bacterial strains used in this study are laboratory strain *P. aeruginosa* PAO1 (Stover et al., 2000) and three clinical CF isolates LMG 27648, LMG 27643, and LMG 27649. These clinical *P. aeruginosa* isolates were obtained from the Belgian Coordinated Collections of Microorganisms (BCCM, Brussels, Belgium). Strains were routinely grown on Mueller Hinton (MH; Oxoid) broth. Artificial sputum media (ASM) and minimal MOPS medium (MMM) were prepared as described elsewhere (Kirchner et al., 2012; LaBauve and Wargo, 2012).

2.3 Minimum inhibitory concentration (MIC)

MIC tests were performed in MH, MMM and ASM using the macro-dilution protocol as described elsewhere (Andrews, 2001). The MIC is defined as the lowest concentration of an antibiotic agent that shows no visible growth of a microorganism after overnight incubation.

2.4 Colony biofilm assay

116   Colony biofilms of *P. aeruginosa* were grown as described (Merritt et al., 2005). Briefly, sterile

117   semipermeable polycarbonate membranes (Whatman, Little Chalfont, UK; 0.2 μm pore size,

118   25 mm) were placed on the surface of MH agar plates. Then an aliquot of 50 μl of overnight

119   culture, adjusted to an optical density (OD) at 600 nm of 0.05, was spotted on each membrane.

120   After that, the inoculated membranes were incubated for 48 h at 37°C to permit biofilm

121   formation. The polycarbonate membranes were moved to fresh agar plates with sterile forceps

122   on a daily basis. On the third day, a 30 μg tobramycin disc (Oxoid), or a glass fibre filter with

123   TIP of various sizes (see section 2.6) were placed on the biofilms using sterile forceps. In case

124   of the glass fibre filter, TIP particles were in direct contact with the top of the biofilms, and

125   controls were covered with a filter without tobramycin. A schematic of the colony biofilm with

126   tobramycin filter is shown in Figure 1. The biofilms were then incubated for a further 3 h or

127   24 h, after which cells were harvested by resuspension in 5 mL of sterile phosphate buffered

128   saline (PBS). Cells were dispersed by vigorously vortexing, and the colony forming units were

129   determined by serial dilution and plating.

130

131   **2.5 Tobramycin capsule filling and humidity control**

132   To collect similar amounts of TIP with different particle sizes, we adjusted the mass of TIP

133   aerosolised into the NGI. Before each experiment, hydroxypropyl methylcellulose capsules

134   (HPMC; transparent; size #3; Capsugel, Colmar, France) were filled manually with TIP

135   extracted from TOBI Podhaler® capsules and weighed using a four-place analytical balance

136   (Sartorius, Epsom, UK). Initial experiments found unacceptable variation in NGI deposition

137   when capsules were filled immediately before use. Therefore, capsules were stored for 24 h in

138   a sealed desiccator under a controlled temperature of 25°C and relative humidity (RH) of 43%

139   before testing, resulting in acceptable reproducibility. This RH was produced using a saturated

140   salt solution of potassium carbonate (K_2CO_3) (Miller et al., 2017). Temperature and relative

141   humidity were monitored using a thermohygrometer placed inside the desiccator, and the

142   following day these capsules were aerosolised through the NGI as described below (section

143   2.6).

144

2.6 Operation of the NGI

146   The NGI was used by applying conditions described elsewhere (Meenach et al., 2013). Briefly,

147   before testing, the pre-separator was filled with 15mL Milli-Q water. The NGI stages were

148   coated with a solution of 1% (v/v) glycerol in methanol (VWR Chemicals) to minimize particle

149   bounce. The NGI was connected to twin vacuum pumps (GAST 1023 series, connected in

150   parallel) via a critical flow controller (TPK, Copley, Nottingham, UK), which was fixed before

151   each experiment at 30 L/min or 60 L/min flow rates using a digital flow meter (DFM2000,

152   Copley Scientific, Nottingham, UK). A TIP capsule for each experiment was aerosolised from

153   a Podhaler through the NGI for 10 seconds, which was chosen as it is sufficient for complete

154   dispersion of the powder from the capsule.

155   Initial experiments were carried out to determine the aerodynamic particle size distribution of

156   TIP when aerosolised from the Podhaler at 30 L/min and 60 L/min. These experiments utilised

157   all eight stages of the NGI and the aerosolization of 28 mg TIP from a single as supplied TOBI

158   capsule (n=5). Following each aerosolization, the mass of tobramycin collected on the

159   induction port, pre-separator, stages 1 to 7, and MOC was determined (section 2.8).

160   Subsequently, TIP particles of different sizes were collected from either stage 2 or 4 using an

161   Aerosol Dose Collection (ADC) device (Price et al., 2020). The ADC allows particles to be

162   collected on a glass fibre filter without the formation of *in situ* agglomerates, which can affect

163   their subsequent dissolution behaviour. In the experimental set up with the ADC, a rubber

164 stopper was placed in the NGI air outlet from stage 2 or stage 4 to disrupt airflow and ensure

165 the collection of all TIP particles on the filter. Second, a glass fibre filter (Copley®, 25 mm

166 diameter, 1 μm pore size) was mounted in the ADC to collect TIP particles. The glass fibre

167 filter was replaced for each repeat of the experiment and the flow rate was adjusted for each

168 experiment after placing the filter in the ADC. These filters were either applied directly to

169 biofilms (section 2.4), particles were visualised by electron microscopy (section 2.7), or the

170 mass of TIP collected was determined (section 2.8).

171

172 2.7 Scanning Electron Microscopy (SEM)

173 To demonstrate that the ADC apparatus had successfully captured TIP particles of different

174 sizes, their geometric particle size distribution was determined using SEM. TIP particles on

175 glass fibre filters were analysed by applying conditions stated elsewhere (Li et al., 2014). TIP

176 samples were fixed into aluminium stubs (Agar Scientific, Stansted, UK) using double-sided

177 adhesive carbon tabs (Agar Scientific). Then, the samples were coated with a thin film of gold

178 using a sputter coater (Sputter Coater S 150B, Edwards, Burgess Hill, UK). The coating process

179 was operated at 1 kV of voltage for 3 min. The images were captured using Jeol SEM (Jeol

180 Jsm-6480LV Scanning Electron Microscope; Jeol Ltd, Welwyn Garden City, UK), and several

181 magnifications levels were used. The captured images were further analysed for geometric

182 particle size determination using the software package ImageJ (Schneider et al., 2012). For

183 every ImageJ analysis, manual particle size measurements were performed, and for every

184 measurement fixed criteria were used: all particles in the given image might be measured, even

185 the small particles in front of large particles; a specific number (100) of particles were selected

186 randomly and the same magnification (x5000) was used for all images. As TOBI Podhaler®

187 particles are spherical (McKeage, 2013), particle size was not sensitive to the direction of

188 measurement, so all diameters were measured in the vertical direction. Particle size

189 distributions were summarised by the median diameter and span, which was defined the

190 difference between the ninetieth and tenth centile diameters, divided by the median diameter.

191

192 **2.8 High Performance Liquid Chromatography-Mass Spectrometry (HPLC-MS)**

193 **quantification**

194 To determine the mass of tobramycin collected on parts of the NGI or glass fibre filters, they

195 were rinsed with known volumes of Milli-Q water and sonicated for 10 min in an ultrasonic

196 water bath to ensure complete dissolution of TIP. To quantify the amount of tobramycin, an

197 HPLC-MS method was developed and validated. The chromatographic system consisted of a

198 pentafluoro phenyl F5 column (2.6 µM, 2.1 x 100 mm; Phenomenex, Macclesfield, UK) as the

199 stationary phase, which was used with a flow rate of 0.3 mL/min at 25°C and an injection

200 volume of 10 µL of each sample was injected in triplicate. The mobile phase involved utilizing

201 two solvents, which were 100% water with 0.1% (v/v) formic acid as solvent A and 100%

202 methanol with 0.1% (v/v) formic acid as solvent B. The proportion of these solvents in the

203 mobile phase was controlled during the analysis by the ultra HPLC instrument. Elution was

204 carried out with 0% mobile phase B for 3 min followed by a linear gradient to 100% B for 7

205 min. The mass spectrometer (Bruker Daltonik GmbH, Bremen, Germany) was operated in

206 electrospray time of flight (ESI) positive-ion MS mode, and the following conditions were used

207 during the MS analysis. The capillary voltage was set to 4500 V, nebulizing gas at 4 bar, and

208 drying gas at 12 L/min at 220°C. The concentration of tobramycin in injected samples (and

209 thus the mass of deposited tobramycin) was determined by constructing a calibration curve

210 using kanamycin as an internal standard. Following the addition of kanamycin (final

211 concentration 4 µg/mL), samples were vigorously vortexed prior to HPLC-MS analysis. All

212   stock solutions were prepared on the same day of the experiment, and HPLC-MS analysis was

213   performed with 24 h. The calibration curve was linear ($r^2 = 0.998$) over the range of 5 to 20

214   µg/ml. Based on the standard deviation of y-intercepts of the regression line (International

215   Conference on Harmonisation, 1996), the estimates for the limit of detection was 1.4 µg/ml

216   and the limit of quantification was 4.4 µg/ml.

217

218   **2.10 Statistical analysis**

219   Data were presented as the mean ± standard error of the mean (SEM) of n ≥ 3 independent

220   biological repeats. Results were analysed using GraphPad Prism 7 by applying the Student *t*-

221   test. Values of *p*< 0.05 were considered statistically significant.

222

3. Results

3.1 The *in vitro* activity of tobramycin against *P. aeruginosa*

The MICs (Table 1) of tobramycin against one laboratory strain (*P. aeruginosa* PAO1) and three clinical CF isolates (*P. aeruginosa* LMG 27648, LMG 27643, and LMG 27649) were determined in MH broth, MMM and ASM by the macro-dilution method. The results showed that MIC values in in MH broth and MMM were fairly similar and differed by at most one doubling dilution, in the range of 0.25-1 µg/mL The MIC was, for all four strains, 4 µg/mL when ASM was used. All strains were susceptible to tobramycin according to BSAC breakpoints.

To determine the activity of tobramycin against *P. aeruginosa* biofilms, which is the state that the cells are in during a lung infection, a colony biofilm assay was used. This model was chosen as the biofilm grow on a semi-solid surface with an air interface, which is probably more representative of biofilms in the lung as compared to the more standard 96-well plate assay in which biofilms are completely immersed in liquid. The results showed that in all tested strains, tobramycin reduced the viable count in the biofilms moderately (Fig 2). However, complete eradication was not achieved and the reduction in viable count was, on average, approximately 60%.

3.2 Aerodynamic particle size distribution of tobramycin inhalation powder

The aerodynamic particle size distributions of TIP aerosolised from the Podhaler at both 30 L/min and 60 L/min are shown in Fig 3.

3.3 Tobramycin masses collected with the ADC mounted on stages 2 or 4 of the NGI

246   To determine the effect of particle size on eradication of *P. aeruginosa* biofilms, it was

247   necessary to collect the same amount of TIP but with different particle sizes. The parameters

248   to obtain approximately 0.5 mg TIP per filter were determined in an empirical manner. To this

249   purpose we used the ADC mounted onto the NGI and determined that, at stage 2 at 30 L/min

250   and TIP capsule mass of 4.4 mg, we collected a very similar mass as when using stage 4 at 60

251   L/min and TIP capsule mass of 4.3 mg. This resulted in a mean mass of 0.51 mg with SD value

252   of 0.05 for larger particles (stage 2 at 30 L/min, d_{ae}<11.7 μm) and 0.48 mg with SD value of

253   0.12 for smaller particles (stage 4 at 60 L/min, d_{ae}<2.82 μm), with a difference between those

254   masses of 7.8%. Statistically, the difference between the masses was not significant (*p*=0.15).

255

256   **3.4 SEM analysis**

257   Before testing fractionated tobramycin particles on biofilms, a number of tests were performed.

258   Firstly, SEM analysis was used to image TIP particles that had been extracted from the NGI

259   stages using the method outlined in section 2.6. These SEM images were further analysed to

260   obtain geometric particle size measurements using ImageJ software. Representative SEM

261   micrographs for TIP particles (Fig 4) show polydisperse, approximately spherical, and porous

262   microparticles. The geometric particle size distributions determined from these images, using

263   ImageJ, were approximately log-normal (Fig 5) and showed that on stage 2 at 30 L/min, the

264   particle size distribution included some coarse particles, with a median geometric diameter of

265   5.6 μm and span of 1.5. The particles collected at stage 4 at 60 L/min had a smaller median

266   geometric diameter of 1.4 μm and span of 1.2.

267

268

3.5 The influence of differently sized tobramycin inhalation powder particles against *P. aeruginosa* biofilms

The fractions of small and large TIP particles were used to challenge *P. aeruginosa* biofilms. These were treated with a dose of 0.5 mg/filter TIP, and filters without tobramycin were used as control. The biofilms were incubated for 3 h, as this period is comparable to the time it takes for tobramycin sputum concentrations to be significantly reduced in people with CF (Hubert et al., 2009; Poli et al., 2007). The 3 h treatment time was not particularly effective in killing cells in our biofilm model but, crucially, there was an approximate 20% reduction of the viable count when applying particles with d_{ae}<2.82 μm as compared with particles with d_{ae}<11.7 μm (Fig 6). For *P. aeruginosa* LMG27649 and LMG27643, particles with d_{ae}<11.7 μm did not have any effect on the biofilms, but there was a statistically significant (LMG27649: p=0.04; LMG27643: p=0.02) reduction with particles with d_{ae}<2.82 μm. For the other two strains, larger particles had a moderate effect on the viable count of cells in biofilms and there was a further reduction in viable count when the biofilms were treated with smaller particles. However, in the latter cases this reduction was statistically not significant (LMG27648: *p*=0.26; PAO1: *p*=0.63).

The reduction in viable count after a 3 h treatment of the biofilms was rather poor, so we also tested the effect of a 24 h incubation with TIP. In this case, the reduction in viable count was between 80-90% when comparing samples with the untreated control (Fig 7). However, there was no significant difference in viable count reduction when comparing small and large TIP particles.

4. Discussion

We investigated the influence of differently sized TIP particles against *P. aeruginosa* biofilms by making use of the NGI to separate particles into different fractions. These particles were collected from stage 2 at 30 L/min and stage 4 at 60 L/min, meaning that the collected fractions had d_{ae}<11.7 µm and d_{ae}<2.82 µm, respectively (Marple et al., 2003). The efficiency of the NGI and ADC device at capturing particles of different size ranges was confirmed by the SEM analysis, which found particles captured at stage 2 at 30 L/min had a larger median geometric diameter (5.6 µm) than those captured at stage 4 at 60 L/min (1.4 µm).

An aerosol collection apparatus was used to collect TIP particles from the above-mentioned stages. Without this, deposition of particles from the NGI occurs directly on a solid impactor stage with high-speed deposition of particles in a small area, which results in the formation of strong agglomerates which then behave as larger particles (Price et al., 2020). However, using the ADC apparatus enables a slow and uniform deposition of aerosol particles over a single, large surface area glass fibre filter, so the collected powder subsequently behaves as single particles.

A difficult issue to resolve was that the NGI separates powder into size fractions with different masses for each fraction, while equal masses were required to analyse the effect of particle size only. Moreover, the amount of tobramycin collected did not vary in a linear fashion with the aerosolised dose, so was difficult to predict. We essentially had to use a trial and error process to determine the parameters to collect equal masses of differently sized particles. Another issue was that initially the mass of TIP collected from the ADC device was variable, but results became more consistent when capsules were equilibrated at a constant humidity and temperature, before use.

When antibiotic particles are deposited on a biofilm, they must first dissolve in order to exert their pharmacological activity. This depends on particle size, which is one of the parameters that determines physical properties of a drug (Shekunov et al., 2007; Wang et al., 2017). Accordingly, the influence of TIP particles was investigated by testing differently sized particles for 3 and 24 h. At 24 h, there was a significant reduction in the viable count when comparing treated with untreated samples, but there was no difference between smaller and larger particles. Thus, over 24 h the difference in the rate of dissolution of small and large TIP particles is not a rate limiting step. However, this time is not physiologically relevant, as tobramycin sputum concentrations are significantly reduced after just 3 h in people with CF (Hubert et al., 2009; Poli et al., 2007), with the TOBI Podhaler having a sputum half-life of only 1-2 hours (Geller et al., 2007). An incubation time of 3 h was thus more appropriate. This time period was far less effective in reducing the viable count but, importantly, smaller particles were more effective by approximately 20% when compared to larger particles. Indeed, it is generally recognized that the dissolution rate of small-sized particles can be significantly better than the larger-sized particles, which is attributed to the larger specific surface area of the small particles (Riley et al., 2012; Tay et al., 2018; van der Wiel et al., 2017; Watts and Williams, 2011). We should note, however, that while we observed a difference in the effectivity between small and large particles for all *P. aeruginosa* strains, it was statistically significant only for the two clinical isolates that were the most recalcitrant to a 3 h treatment, (LMG27649 and LMG27643). In these strains, larger particles did not cause any reduction in the viable count, while small particles resulted in a 20% reduction. In case of the other strains (LMG27648 and PAO1), larger particles resulted in approximately 15-20% reduction in viable count, with a further non-significant reduction with smaller particles. Planktonic cells of those four strains all displayed the same sensitivity to tobramycin, but phenotypic and genetic differences between the strains could result in the differences in biofilm formation, such as in composition

339   of the extracellular matrix or thickness of the biofilms (Wimpenny et al., 2000). For example,

340   the three clinical isolates are reported to be alginate producers (Hoffmann et al., 2005; Leitão

341   et al., 1996; Mathee et al., 2008), whereas the laboratory strain PAO1 does not produce this

342   polysaccharide. We also observed that only LMG 27649 was unable to grow in a minimal

343   growth medium without the addition of casamino acids (data not shown), indicating that this

344   strain is auxotrophic, whereas the other strains are not. Whether this would influence the effects

345   of tobramycin particles is not known, but it does clearly show that the strains differ from each

346   other.

347   The influence of differently sized particles of other drugs has been evaluated previously,

348   showing better efficacy for smaller sized particles as compared to larger (Jinno et al., 2006;

349   Leach et al., 2009; Liu et al., 2015). For example, for the oral vasodilator cilostazol, smaller

350   cilostazol particles of 2.4 µm had a better rate of dissolution and efficacy than particles of 13

351   µm (Jinno et al., 2006). This was also observed for inhaled beclomethasone (a corticosteroid),

352   which is more effective in a particle size of 1.1 µm as compared to 4 µm (Leach et al., 2009;

353   Van Schayck and Donnell, 2004; Vanden Burgt et al., 2000). Although these differences have

354   been attributed to varying lung deposition patterns with changing particle size, they may also

355   have been influenced the faster dissolution rate of smaller particles.

356   We should acknowledge that our study has limitations. Firstly, there was a slight difference in

357   the TIP mass that were collected for small and large sized particles from different stages/flow

358   rates. It was technically difficult to obtain equal masses of differently sized particles, in

359   particular at the amounts required for biofilm assays (0.5 mg/filter). However, the difference

360   in the amounts obtained was statistically not significant ($p > 0.05$). It should be noted that on

361   average we collected slightly less (<8%) of the smaller particles, but these were nevertheless

362   more effective, which only strengthens our conclusion that smaller particle sizes result in more

363   efficient killing of cells in *P. aeruginosa* biofilms.

Another limitation is that with the NGI the maximum particle size that is collected on the filters can be controlled, but not the minimum particle size. Thus, while the average particle size differs between the collected fractions, there is some overlap in particle sizes and effects on antibiofilm activity could have been greater if it was technically possible to control both minimum and maximum sizes. Also, our SEM analysis only measured the diameters of a small number of particles (100). Despite this, we obtained log-normal particle size distributions (Fig 5), so these data provide additional reassurance that the NGI and ADC device collected particles of different sizes.

Our system used the *in vitro* colony biofilm model (Merritt et al., 2005). It is a simple model system but nevertheless it is useful as biofilm grows on a semi-solid surface with an air-interface. It is of course not the same as the conditions found in a lung, but in this study, it was a more useful model than for instance the standard 96-well plate biofilm assay. It should also be noted that 0.5 mg/filter TIP as used here is actually a very large dose when compared to a therapeutic dose of 112 mg spread through the whole surface area of the lungs (Geller et al., 2011). Future studies therefore need to focus on the use of models that, firstly, use an amount of antibiotic that better reflects clinical doses and, secondly, better mimic the *in vivo* lung pathological conditions. The latter could be achieved using, for instance, *ex vivo* models that use porcine lung samples (Harrison and Diggle, 2016), or *in vivo* models (Kukavica-Ibrulj and Levesque, 2008).

Our hypothesis on the effect of particle size was only tested for one dry powder inhaled antibiotic, tobramycin. An important aim of our study was to establish a system to test dry powder inhalers on biofilms. This has now been achieved and has demonstrated that the particle size of inhaled dry powders can influence their anti-biofilm activity. These are the most significant aspects of these findings, as this tool can be used to test other antibiotics. Our system may be of particular relevance to the development of dry powder inhaled formulations of drugs

389 with a low aqueous solubility, as in this situation the differences between small and large

390 particles may become more pronounced than for tobramycin (which is freely soluble in water).

391 Investigation of this issue may therefore highlight additional ways to increase the effectiveness

392 of poorly soluble inhaled drugs. Future research should also measure the dissolution rate of

393 different antibiotic particle size fractions, to fully examine the potential relationship between

394 anti-biofilm activity and particle dissolution.

395 **5. Conclusion**

396 Tobramycin dry powder inhaler is one of the most widely used inhaled antibiotics in the

397 treatment of CF lung infections. Here we showed that small TIP particles (d_{ae}<2.82 µm)

398 showed better efficacy as indicated by a 20% reduction in the viable count as compared to

399 larger particles (d_{ae}<11.7 µm) at an incubation time of 3 h against *P. aeruginosa* biofilms; this

400 reduction was statistically significant for two strains of the four strain, but the trend was

401 observed in all strains. This short incubation time is important, as this is the same timeframe in

402 which tobramycin is largely cleared from the lung. These initial findings highlight that particle

403 size can affect TIP antibiofilm activity. Importantly, we have developed a system to test the

404 effect of dry powder inhalers on bacterial biofilms, and we are planning to utilise this to test

405 other antibiotics and as well as employing more advanced biofilm models.

406

References

410

Akkerman-Nijland, A.M., Yousofi, M., Rottier, B.L, van der Vaart, H., Burgerhof, J.G.M.,

411

Frijlink, H.W., Touw D.J., Koppelman G.H., Akkerman, O.W., 2020. Eradication of

412

Pseudomonas aeruginosa in cystic fibrosis patients with inhalation of dry powder

413

tobramycin. Ther Adv Respir Dis. 14, 1753466620905279

414

Ambrus, R., Benke, E., Farkas, A., Balashazy, I., Szabo-Revesz, P., 2018. Novel dry powder

415

inhaler formulation containing antibiotic using combined technology to improve aerodynamic

416

properties. Eur. J. Pharm. Sci. 123, 20-27.

417

Andrews, J.M., 2001. Determination of minimum inhibitory concentrations. J. Antimicrob.

418

Chemother. 48 Suppl 1, 5-16.

419

Buttini, F., Brambilla, G., Copelli, D., Sisti, V., Balducci, A.G., Bettini, R., Pasquali, I., 2016.

420

Effect of flow rate on in vitro aerodynamic performance of NEXThaler® in comparison with

421

Diskus® and Turbohaler® dry powder inhalers. J. Aerosol Med. Pulm. Drug Deliv. 29, 167-

422

178.

423

Ciofu, O., Tolker-Nielsen, T., Jensen, P.O., Wang, H., Hoiby, N., 2015. Antimicrobial

424

resistance, respiratory tract infections and role of biofilms in lung infections in cystic fibrosis

425

patients. Adv. Drug. Deliv. Rev. 85, 7-23.

426

Deng, Q., Ou, C., Chen, J., Xiang, Y., 2018. Particle deposition in tracheobronchial airways of

427

an infant, child and adult. Sci. Total Environ. 612, 339-346.

428

Furiga, A., Lajoie, B., El Hage, S., Baziard, G., Roques, C., 2015. Impairment of *Pseudomonas*

429

aeruginosa biofilm resistance to antibiotics by combining the drugs with a new quorum-

430

sensing inhibitor. Antimicrob. Agents Chemother. 60, 1676-1686.

431

Geller, D.E., Konstan, M.W., Smith, J., Noonberg, S., Conrad, C., 2007. Novel Tobramycin

432

Inhalation Powder in Cystic Fibrosis Subjects: Pharmacokinetics and Safety. Pediatr Pulmonol

433

42, 307-313.

434

435 Geller, D.E., Weers, J., Heuerding, S., 2011. Development of an inhaled dry-powder

436 formulation of tobramycin using PulmoSphere technology. J. Aerosol Med. Pulm. Drug Deliv.

437 24, 175-182.

438 Guo, C., Gillespie, S.R., Kauffman, J., Doub, W.H., 2008. Comparison of delivery

439 characteristics from a combination metered-dose inhaler using the Andersen cascade impactor

440 and the next generation pharmaceutical impactor. J. Pharm. Sci. 97, 3321-3334.

441 Harrison, F., Diggle, S.P., 2016. An ex vivo lung model to study bronchioles infected with

442 *Pseudomonas aeruginosa* biofilms. Microbiology 162, 1755-1760.

443 Harrison, M.J., McCarthy, M., Fleming, C., Hickey, C., Shortt, C., Eustace, J.A., Murphy,

444 D.M., Plant, B.J. 2014. Inhaled versus nebulised tobramycin: a real world comparinson in adult

445 cystic fibrosis (CF). J. Cyst. Fibros. 13, 692-698.

446 Hoffmann, N., Rasmussen, T.B., Jensen, P.O., Stub, C., Hentzer, M., Molin, S., Ciofu, O.,

447 Givskov, M., Johansen, H.K., Hoiby, N., 2005. Novel mouse model of chronic *Pseudomonas*

448 *aeruginosa* lung infection mimicking cystic fibrosis. Infect. Immun. 73, 2504-2514.

449 Hoiby, N., 2011. Recent advances in the treatment of *Pseudomonas aeruginosa* infections in

450 cystic fibrosis, BMC Med., 9, 32.

451 Hubert, D., Leroy, S., Nove-Josserand, R., Murris-Espin, M., Mely, L., Dominique, S., Delaisi,

452 B., Kho, P., Kovarik, J.M., 2009. Pharmacokinetics and safety of tobramycin administered by

453 the PARI eFlow® rapid nebulizer in cystic fibrosis. J Cyst Fibros 8, 332-337.

454 International Conference on Harmonization (ICH) of Technical Requirements for the

455 Registration of Pharmaceuticals for Human Use, 1996. Validation of analytical procedures:

456 Text and Methodology. ICH-Q2B, Geneva.

457 Jinno, J.-i., Kamada, N., Miyake, M., Yamada, K., Mukai, T., Odomi, M., Toguchi, H.,

458 Liversidge, G.G., Higaki, K., Kimura, T., 2006. Effect of particle size reduction on dissolution

459 and oral absorption of a poorly water-soluble drug, cilostazol, in beagle dogs. J. Control.

460 Release 111, 56-64.

461 Kirchner, S., Fothergill, J.L., Wright, E.A., James, C.E., Mowat, E., Winstanley, C., 2012. Use

462 of artificial sputum medium to test antibiotic efficacy against *Pseudomonas aeruginos*a in

463 conditions more relevant to the cystic fibrosis lung, J. Vis. Exp., e3857-e3857.

464 Konstan, M.W., Flume, P.A., Kappler, M., Chiron, R., Higgins, M., Brockhaus, F., Zhang, J.,

465 Angyalosi, G., He, E., Geller, D.E., 2011. Safety, efficacy and convenience of tobramycin

466 inhalation powder in cystic fibrosis patients: The EAGER trial. J. Cyst. Fibros. 10, 54-61.

467 Kukavica-Ibrulj, I., Levesque, R.C., 2008. Animal models of chronic lung infection with

468 *Pseudomonas aeruginosa*: useful tools for cystic fibrosis studies. Lab. Anim. 42, 389-412.

469 LaBauve, A.E., Wargo, M.J., 2012. Growth and laboratory maintenance of *Pseudomonas*

470 *aeruginosa*. Curr. Protoc. Microbiol. 25, 6E.1.1-6E.1.8.

471 Leach, C., Colice, G.L., Luskin, A., 2009. Particle size of inhaled corticosteroids: Does it

472 matter? J. Allergy Clin. Immunol. 124, S88-S93.

473 Leitão, J.H., Alvim, T., Sá-Correia, I., 1996. Ribotyping of *Pseudomonas aeruginosa* isolates

474 from patients and water springs and genome fingerprinting of variants concerning mucoidy.

475 FEMS Immunol. Med. Microbiol. 13, 287-292.

476 Li, X., Vogt, F.G., Hayes, D., Jr., Mansour, H.M., 2014. Design, characterization, and aerosol

477 dispersion performance modeling of advanced co-spray dried antibiotics with mannitol as

478 respirable microparticles/nanoparticles for targeted pulmonary delivery as dry powder inhalers.

479 J. Pharm. Sci. 103, 2937-2949.

480 Liu, D., Pan, H., He, F., Wang, X., Li, J., Yang, X., Pan, W., 2015. Effect of particle size on

481 oral absorption of carvedilol nanosuspensions: in vitro and in vivo evaluation. Int. J.

482 Nanomedicine 10, 6425-6434.

483 Marple, V., Roberts, D., Romay, F., C Miller, N., G Truman, K., Van Oort, M., Olsson, B., J

484 Holroyd, M., Mitchell, J., Hochrainer, D., 2003. Next Generation Pharmaceutical Impactor (A

485 New Impactor for Pharmaceutical Inhaler Testing). Part I: Design. J. Aerosol Med. Pulm. Drug

486 Deliv. 16, 283-299.

487 Marshall, L.J., Oguejiofor, W., Price, R., Shur, J., 2016. Investigation of the enhanced

488 antimicrobial activity of combination dry powder inhaler formulations of lactoferrin. Int. J.

489 Pharm. 514, 399-406.

490 Mathee, K., Narasimhan, G., Valdes, C., Qiu, X., Matewish, J.M., Koehrsen, M., Rokas, A.,

491 Yandava, C.N., Engels, R., Zeng, E., Olavarietta, R., Doud, M., Smith, R.S., Montgomery, P.,

492 White, J.R., Godfrey, P.A., Kodira, C., Birren, B., Galagan, J.E., Lory, S., 2008. Dynamics of

493 *Pseudomonas aeruginosa* genome evolution. Proc. Natl. Acad. Sci. U. S. A. 105, 3100-3105.

494 McKeage, K., 2013. Tobramycin inhalation powder: a review of its use in the treatment of

495 chronic *Pseudomonas aeruginosa* infection in patients with cystic fibrosis. Drugs 73, 1815-

496 1827.

497 Meenach, S.A., Vogt, F.G., Anderson, K.W., Hilt, J.Z., McGarry, R.C., Mansour, H.M., 2013.

498 Design, physicochemical characterization, and optimization of organic solution advanced

499 spray-dried inhalable dipalmitoylphosphatidylcholine (DPPC) and

500 dipalmitoylphosphatidylethanolamine poly(ethylene glycol) (DPPE-PEG) microparticles and

501 nanoparticles for targeted respiratory nanomedicine delivery as dry powder inhalation aerosols.

502 Int J Nanomedicine 8, 275-293.

503 Merritt, J.H., Kadouri, D.E., O'Toole, G.A., 2005. Growing and analyzing static biofilms, Curr.

504 Protoc. Microbiol., Ch 1, Unit-1B.1.

505 Miller, D.P., Tan, T., Nakamura, J., Malcolmson, R.J., Tarara, T.E., Weers, J.G., 2017.

506 Physical characterization of tobramycin inhalation powder: II. State diagram of an amorphous

507 engineered particle formulation. Mol. Pharm. 14, 1950-1960.

508   Muheim, C., Gotzke, H., Eriksson, A.U., Lindberg, S., Lauritsen, I., Norholm, M.H.H., Daley,

509   D.O., 2017. Increasing the permeability of *Escherichia coli* using MAC13243, Sci. Rep. 7,

510   17629.

511   Nafee, N., Husari, A., Maurer, C.K., Lu, C., de Rossi, C., Steinbach, A., Hartmann, R.W., Lehr,

512   C.M., Schneider, M., 2014. Antibiotic-free nanotherapeutics: ultra-small, mucus-penetrating

513   solid lipid nanoparticles enhance the pulmonary delivery and anti-virulence efficacy of novel

514   quorum sensing inhibitors. J. Control. Release 192, 131-140.

515   Nikaido, H., Pagès, J.-M., 2012. Broad-specificity efflux pumps and their role in multidrug

516   resistance of Gram-negative bacteria. FEMS Microbiol. Rev. 36, 340-363.

517   Patton, J.S., Brain, J.D., Davies, L.A., Fiegel, J., Gumbleton, M., Kim, K.J., Sakagami, M.,

518   Vanbever, R., Ehrhardt, C., 2010. The particle has landed - characterizing the fate of inhaled

519   pharmaceuticals. J. Aerosol Med. Pulm. Drug Deliv. 23 Suppl 2, S71-87.

520   Poli, G., Acerbi, D., Pennini, R., Raschini, A.S., Carrado, M.E., Eichler, H.G., Eichler, I., 2007.

521   Clinical Pharmacology Study of Bramitob®, a Tobramycin Solution for Nebulization, in

522   Comparison with Tobi®. Pediatr. Drugs. 9 Suppl 1, 3-9.

523   Price, R., Shur, J., Ganley, W., Farias, G., Fotaki, N., Conti, D.S., Delvadia, R., Absar, M.,

524   Saluja, B., Lee, S., 2020. Development of an Aerosol dose Collection Apparatus for in vitro

525   dissolution measurements of orally inhaled drug products. AAPS J 22, 47.

526   Riley, T., Christopher, D., Arp, J., Casazza, A., Colombani, A., Cooper, A., Dey, M., Maas, J.,

527   Mitchell, J., Reiners, M., Sigari, N., Tougas, T., Lyapustina, S., 2012. Challenges with

528   developing in vitro dissolution tests for orally inhaled products (OIPs). AAPS PharmSciTech

529   13, 978-989.

530   Roberts, D.L., Mitchell, J.P., 2013. The effect of nonideal cascade impactor stage collection

531   efficiency curves on the interpretation of the size of inhaler-generated aerosols. AAPS

532   PharmSciTech 14, 497-510.

533   Rowland, M., Cavecchi, A., Thielmann, F., Kulon, J., Shur, J., Price, R., 2018. Measuring the

534   bipolar charge distributions of fine particle aerosol clouds of commercial PMDI suspensions

535   using a bipolar Next Generation Impactor (bp-NGI). Pharm. Res. 36, 15.

536   Schneider, C.A., Rasband, W.S., Eliceiri, K.W., 2012. NIH Image to ImageJ: 25 years of image

537   analysis. Nat. Methods 9, 671-675.

538   Shah, P.L., Scott, S.F., Geddes, D.M., Conway, S., Watson, A., Nazir, T., Carr, S.B., Wallis,

539   C., Marriott, C., Hodson, M.E., 1997. An evaluation of two aerosol delivery systems for

540   rhDNase. Eur. Respir. J. 10, 1261-1266.

541   She, P., Wang, Y., Luo, Z., Chen, L., Tan, R., Wang, Y., Wu, Y., 2018. Meloxicam inhibits

542   biofilm formation and enhances antimicrobial agents efficacy by *Pseudomonas aeruginosa*,

543   Microbiologyopen, 7, e00545.

544   Shekunov, B.Y., Chattopadhyay, P., Tong, H.H.Y., Chow, A.H.L., 2007. Particle size analysis

545   in pharmaceutics: principles, methods and applications. Pharm. Res. 24, 203-227.

546   Stover, C.K., Pham, X.Q., Erwin, A.L., Mizoguchi, S.D., Warrener, P., Hickey, M.J.,

547   Brinkman, F.S., Hufnagle, W.O., Kowalik, D.J., Lagrou, M., Garber, R.L., Goltry, L.,

548   Tolentino, E., Westbrock-Wadman, S., Yuan, Y., Brody, L.L., Coulter, S.N., Folger, K.R., Kas,

549   A., Larbig, K., Lim, R., Smith, K., Spencer, D., Wong, G.K., Wu, Z., Paulsen, I.T., Reizer, J.,

550   Saier, M.H., Hancock, R.E., Lory, S., Olson, M.V., 2000. Complete genome sequence of

551   *Pseudomonas aeruginosa* PAO1, an opportunistic pathogen. Nature 406, 959-964.

552   Tay, J.Y.S., Liew, C.V., Heng, P.W.S., 2018. Dissolution of fine particle fraction from

553   truncated Anderson Cascade Impactor with an enhancer cell. Int. J. Pharm. 545, 45-50.

554   Tiddens, H.A., Bos, A.C., Mouton, J.W., Devadason, S., Janssens, H.M., 2014. Inhaled

555   antibiotics: dry or wet? Eur. Respir. J. 44, 1308-1318.

556 van der Wiel, E., Lexmond, A.J., van den Berge, M., Postma, D.S., Hagedoorn, P., Frijlink,

557 H.W., Farenhorst, M.P., de Boer, A.H., Ten Hacken, N.H.T., 2017. Targeting the small airways

558 with dry powder adenosine: a challenging concept, Eur Clin Respir J, 4, 1369328.

559 Van Schayck, C.P., Donnell, D., 2004. The efficacy and safety of QVAR (hydrofluoroalkane-

560 beclometasone diproprionate extrafine aerosol) in asthma (Part 2): Clinical experience in

561 children. Int. J. Clin. Pract. 58, 786-794.

562 Vanden Burgt, J.A., Busse, W.W., Martin, R.J., Szefler, S.J., Donnell, D., 2000. Efficacy and

563 safety overview of a new inhaled corticosteroid, QVAR (hydrofluoroalkane-beclomethasone

564 extrafine inhalation aerosol), in asthma. J. Allergy Clin. Immunol. 106, 1209-1226.

565 Verbanck, S., Schuermans, D., Paiva, M., Vincken, W., 2006. The functional benefit of anti-

566 inflammatory aerosols in the lung periphery. J. Allergy Clin. Immunol. 118, 340-346.

567 Wang, H., Bhambri, P., Ivey, J., Vehring, R., 2017. Design and pharmaceutical applications of

568 a low-flow-rate single-nozzle impactor. Int. J. Pharm. 533, 14-25.

569 Watts, A.B., Williams, R.O., 2011. Nanoparticles for Pulmonary Delivery, in: Smyth, H.D.C.,

570 Hickey, A.J. (Eds.), Controlled Pulmonary Drug Delivery. Springer, New York, NY, pp. 335-

571 366.

572 Wimpenny, J., Manz, W., Szewzyk, U., 2000. Heterogeneity in biofilms. FEMS Microbiol.

573 Rev. 24, 661-671.

574 Worlitzsch, D., Tarran, R., Ulrich, M., Schwab, U., Cekici, A., Meyer, K.C., Birrer, P., Bellon,

575 G., Berger, J., Weiss, T., Botzenhart, K., Yankaskas, J.R., Randell, S., Boucher, R.C., Doring,

576 G., 2002. Effects of reduced mucus oxygen concentration in airway *Pseudomonas* infections

577 of cystic fibrosis patients. J. Clin. Invest. 109, 317-325.

578

579   Table 1. The MICs (μg/mL) of tobramycin against *P. aeruginosa* clinical CF isolates and

580   PAO1 determined in triplicate by macro-dilution method in MH, MMM and ASM media.

581

P. aeruginosa strain	MICs in MH	MIC in MMM	MICs in ASM
LMG 27649	0.5	1	4
LMG 27643	0.5	0.25	4
LMG 27648	1	0.5	4
PAO1	0.5	0.5	4

582

583

584

585

586

587

Figure legends

Figure 1. Schematic of the colony biofilm. Cells were grown on a polycarbonate membrane to form a biofilm, and on the third day a filter with tobramycin inhalation powder was placed on top. After incubation for 3 or 24 hours, the cells were harvested and a viable count was determined.

Figure 2. The *in vitro* activity of tobramycin against *P. aeruginosa* using the colony biofilm assay. (A – C) show clinical CF isolates and (D) indicates laboratory strain PAO1. All *P. aeruginosa* biofilms were grown for 48 h on MH agar, treated with 30 µg/disc tobramycin, and incubated for 24 h at 37°C. The controls represent biofilms without tobramycin. The data shown represent the standard error of the mean from three biological repeats and each biological repeat consisted of at least two technical repeats. Statistics were analysed using unpaired 2-tailed *t* test. Statistically significant differences between treated biofilms (***, $p<0.001$; ****, $p<0.0001$) and the control are indicated.

Figure 3. Aerosol particle size distribution of tobramycin inhalation powder when aerosolised for 10 seconds from the Podhaler® device into the NGI at 30 L/min (A) and 60 L/min (B). Error bars represent the standard error of the mean from five independent experiments for each flow rate. Stages 1-7 indicate the impactor stages, followed by their corresponding cut off aerodynamic diameter in parentheses. MOC: micro-orifice collector.

Figure 4. Representative SEM micrographs of TIP particles from NGI stages at different flow rates. Stage 2, at 30 L/min (A) and Stage 4, at 60 L/min (B). Pictures were taken at x4,000 magnification (scale bar = 5 µm).

Figure 5. Comparison of the cumulative geometric particle size distributions of tobramycin inhalation powder particles collected at stage 2 (A) and 4 (B) of the NGI at 30 L/min and 60 L/min, respectively.
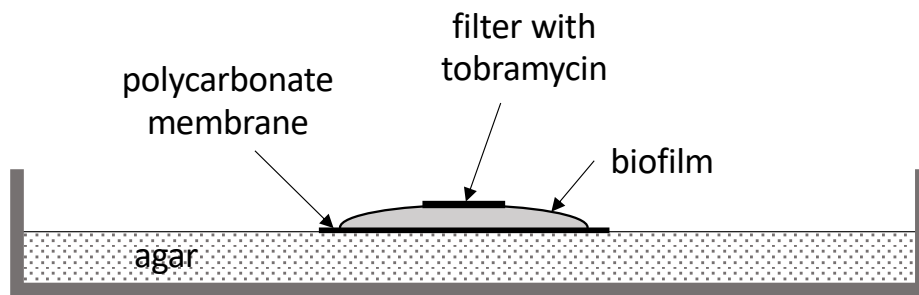
612 **Figure 6.** The influence of differently size TIP particles on the eradication of *P. aeruginosa*

613 biofilms. (A-C) show clinical isolates, and (D) indicates the laboratory strain PAO1. Bacterial

614 cells were grown as colony biofilms for 48 h at 37°C and then were treated with different

615 tobramycin particle size fractions of d_{ae}<11.7 μm and d_{ae}<2.82 μm for 3 h. The data shown

616 represent the standard error of the mean from three biological repeats and each biological repeat

617 consisted of at least two technical repeats. Statistics were analysed using an unpaired 2-tailed

618 *t* test. Statistically significant differences between large and small particles are indicated (*,

619 *p*<0.05).

620 **Figure 7.** The influence of differently sized TIP particles on the eradication of *P. aeruginosa*

621 biofilms. (A-C) show clinical isolates, and (D) indicates the laboratory strain PAO1. Bacterial

622 cells were grown as colony biofilms for 48 h at 37°C and then were treated with different

623 tobramycin particle size fractions of d_{ae}<11.7 μm and d_{ae}<2.82 μm for 24 h. The data shown

624 represent the standard error of the mean from three biological repeats and each biological repeat

625 consisted of at least two technical repeats. Statistical significance was analysed using an
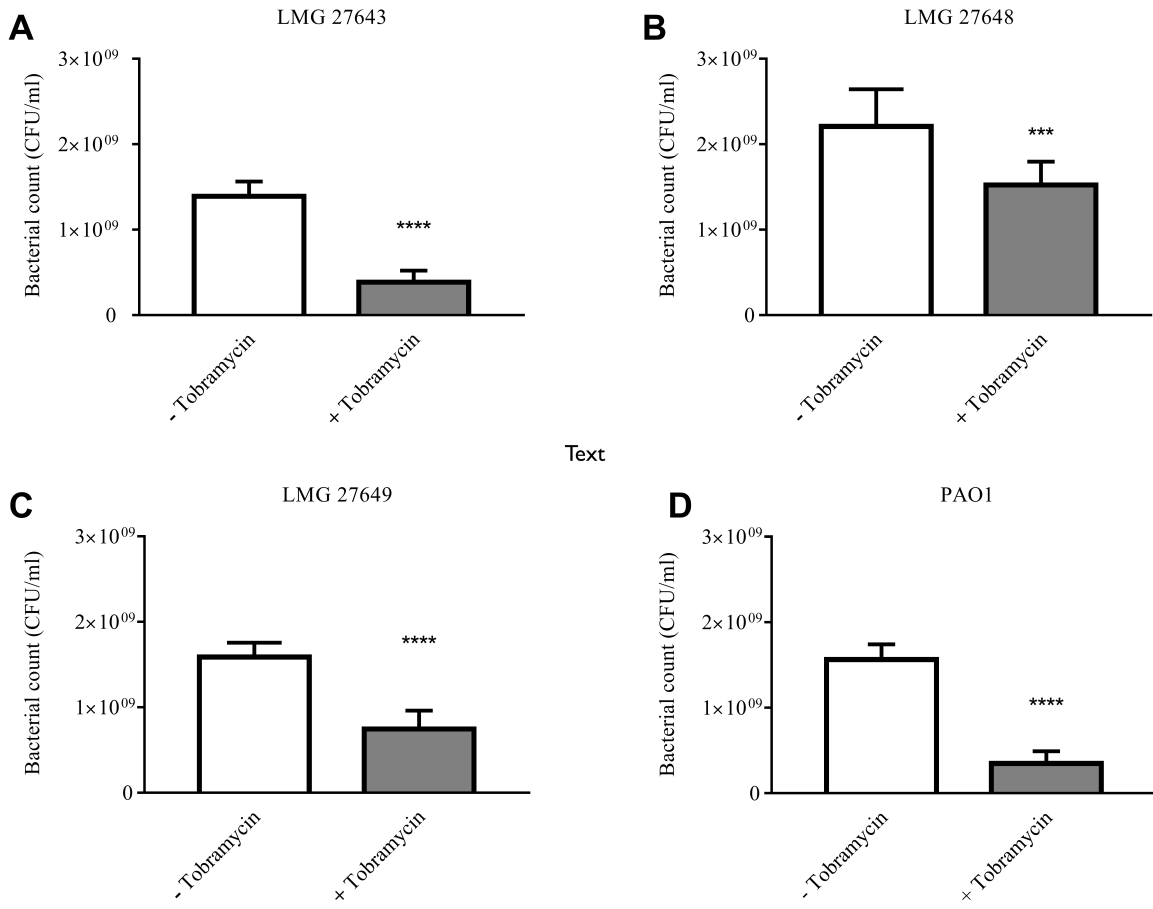
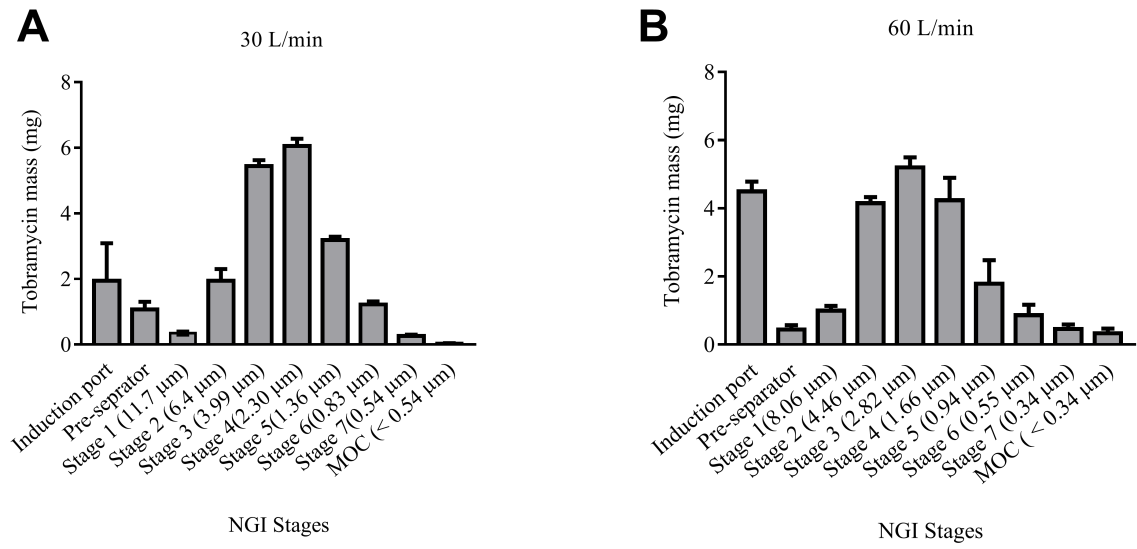626 unpaired 2-tailed *t* test.

627

Figures

630   Figure 1

631

632

633   Figure 2

636   Figure 3
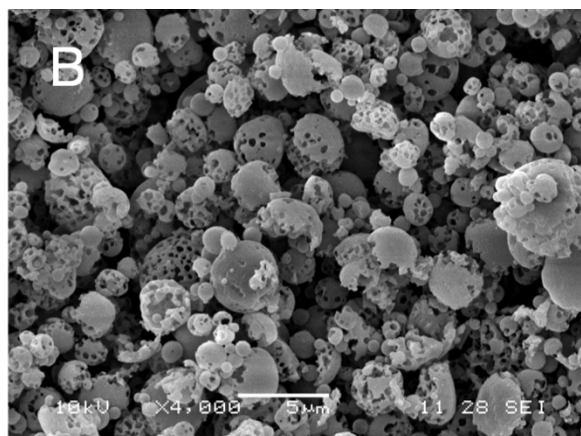

A

30 L/min

Tobramycin mass (mg)

NGI Stages

Induction port, Pre-seprator, Stage 1 (11.7 μm), Stage 2 (6.4 μm), Stage 3 (3.99 μm), Stage 4(2.30 μm), Stage 5(1.36 μm), Stage 6(0.83 μm), Stage 7(0.54 μm), MOC (< 0.54 μm)

B

60 L/min

Tobramycin mass (mg)

NGI Stages

Induction port, Pre-separator, Stage 1(8.06 μm), Stage 2 (4.46 μm), Stage 3 (2.82 μm), Stage 4 (1.66 μm), Stage 5 (0.94 μm), Stage 6 (0.55 μm), Stage 7 (0.34 μm), MOC (< 0.34 μm)

637

638

639

640

641

642   Figure 4

643

644

645

646

647

648   Figure 5

649

A Particle size distribution
stage 2, 30 l/min

B Particle size distribution
stage 4, 60 l/min

650

651

A LMG 27649

B LMG 27643

C LMG 27648

D PAO1

653

654   Figure 7

A   LMG 27649

B   LMG 27643

C   LMG 27648

D   PAO1

655

656